Smart Geotechnics for Smart Societies – Zhussupbekov, Sarsembayeva & Kaliakin (Eds)

Coupled CFD-DEM simulation of progressive failure of tunnel face

C. Zhou & J.G. Qian*
Tongji University, Shanghai, China

Z.Y. Yin
The Hong Kong Polytechnic University, Hong Kong, China

ABSTRACT: Extensive studies have been conducted to investigate the face stability of tunnelling by the discrete element method (DEM). However, the DEM simulation of tunnel face's failure considering water-soil interaction has not yet been available. In this paper, the coupled CFD-DEM method was adopted to simulate the progressive failure of the shield tunnel face in saturated sand, and the tunnel's failure in dry sand was also simulated for comparison. The dynamic mesh method was introduced to accurately simulate the CFD domain's variation due to the movement of the tunnel's face. The excavation face was moved forward or backward at a uniform displacement rate to simulate a passive or active failure, respectively. The ground surface movement and supporting force of tunnel face were analyzed to investigate the feature of tunnel face failure in saturated and dry sandy soils.

1 INTRODUCTION

The shield tunneling method is widely used in urban underground tunneling projects. Inadequate or excessive support forces on the tunnel face may cause tunnel destabilization(Peila, 1994; Mollon, Dias and Soubra, 2011). In the vicinity of the tunnel face, where soil deformation or even soil collapse may take place, it greatly challenges traditional continuous medium methods to reproduce the process of such a progressive failure. Thus the discrete element methods (DEM) were introduced to simulate the large deformation and soil transport. Nevertheless, previous discrete element numerical simulations fail to enable us to well understand water-soil interaction and commonly simulate tunneling in dry sand. The saturated soil involves water-soil interaction, which is a multidisciplinary process governed by the principles of soil mechanics and hydraulics. Therefore, a combination of computational fluid dynamics (CFD) and the discrete element method (DEM) is more appropriate to consider saturated sandy soils.

This paper simulates the progressive failure of shield tunnel face in saturated sand using coupled CFD-DEM method. By analyzing the surface displacement and face support force, the different failure behaviors of tunnel face in saturated and dry ground are revealed.

2 METHODOLOGY AND MODEL SETUP

2.1 *Governing equations*

In CFD-DEM method, the motion of the solid particles is governed by Newton's laws, while the velocity and pressure of fluid are calculated by the volume-averaged Navier-Stokes equations (Kloss *et al.*, 2012):

*Corresponding author:

DOI: 10.1201/9781003299127-125

$$m_i \frac{dv_i}{dt} = \sum_{j=1}^{j=n} F_{ij}^n + \sum_{j=1}^{j=n} F_{ij}^t + F_i^f + F_i^g \tag{1}$$

$$I_i \frac{d\omega_i}{dt} = \sum_{j=1}^{j=n} M_{ij} \tag{2}$$

$$\left(\partial \alpha_f\right)/\partial t + \nabla \cdot \left(\alpha_f u_f\right) = 0 \tag{3}$$

$$\frac{\partial \alpha_f u_f}{\partial t} + \nabla \cdot \alpha_f u_f u_f = -\alpha_f \nabla \frac{p}{\rho_f} - R_{pf} + \nabla \cdot \left(\alpha_f \tau\right) \tag{4}$$

where the particle index is denoted by subscript i; m_i is the particle's mass; v_i and ω_i represents the translational and angular velocity; F_{ij} is the inter-particle contact force while F_i^f is the particle-fluid force; F_i^g is the gravity of each particle; α_f is the fluid volume fraction; u_f and p denotes the fluid velocity and pressure, respectively; ρ_f is fluid density; τ represents the shear stress tensor of the fluid cell; R_{pf} is the exchange of momentum with the particulate phase.

2.2 *Model setup*

Spherical particles are adopted in the DEM simulation. The particle size distribution refers to that used in the previous study (Yin, Wang and Zhang, 2020). The particle size is enlarged by ten times to reduce the number of particles and satisfy computional power requirements, which is commonly adopted in DEM simulations. The largest and smallest particle sizes in the simulation are 30.7mm and 12.2mm, respectively. Some of the particle-related parameters are shown in Table 1. Four tests are carried out with the same model size, and both the dry and saturated surrounding soils are considered in this study. The excavation of the tunnel is simulated by the forward and backward movement of a rigid wall in the DEM. Due to the simulation situation's symmetry, half of the tunnel model is used to save computational resources (as shown in Figure 1). In addition, the gravitational acceleration used in the simulation has been magnified by a factor of 10, with reference to the centrifuge test method (Yin, Wang and Zhang, 2020). The actual size of the prototype is ten times the size set in the model. According to the similarity criterion, the corresponding fluid viscosity coefficients are scaled up by the same. Due to the complexity of excavation speed control in actual projects, this paper simplifies active and passive failure into two cases: tunnel backward and forward. As with previous numerical simulations and tests, the tunnel excavation speed is set to a constant speed of 0.01m/s for forward and backward movement to meet the quasi-static requirements. The total simulation time is the 20s, and the total distance of the forward and backward movements is 200mm.

Table 1. Parameters used in the simulations.

Particle density (kg/m^3)	2650
Young's modulus (MPa)	5×10^8
Poisson's ratio	0.3
Inter-particle friction coefficient	0.5
Rolling friction coefficient	0.1
Timestep (s)	2×10^{-5}
Restitution coefficient	0.3

3 RESULTS ANALYSIS

3.1 *Soil displacement field*

Figure 2 shows the particle displacement distribution in four tests with different tunnel movements (40mm, 100mm, 170mm, and 200mm). The particles with displacement less than a certain value (0.04m) are hidden in the figure. Firstly, for the active failure mode of the tunnel face, it can be seen from Figure 2(a)-(b) that the shapes of the displacement field in the dry sand and saturated sand cases are similar while the area of the destabilization zone in the dry sand is larger than that in the saturated sand. The destabilization angle in saturated sand (57.89°) is slightly larger than that in dry sand (52.56°). For passive failure, as shown in Figure 2(c)-(d), the destabilization zone reaches the ground surface in both cases of dry and saturated sand soils. In addition, it's found there is little difference in the size of the instability zone at the beginning of the tunnel face movement (40 mm, 100 mm). As the test proceeds, a significant difference occurs and the destabilization zone in the saturated sand is significantly larger than that in the dry sand.

3.2 *Ground surface displacement*

Surface displacements caused by tunnel excavation may affect nearby buildings, which has been one of the main concerns for urban tunnel construction. Figure 3(a)-(b) shows the surface displacements corresponding to backward movement (the selected location is X=0, -1.25<Y<1.25). It can be observed that the surface settlement increases with the movement of the tunnel and reaches its maximum value at the end of the test. The maximum settlement in dry sand occurs at -0.117 m from the initial position of the tunnel excavation surface (Y=0.95m), and the settlement value decreases rapidly on both sides of the maximum settlement, showing a "V" shape in the figure. The maximum settlement in saturated sand occurs at Y=1.054m, which is not significantly different from that of dry sand. In contrast, both sides' settlement decreases more slowly, and the overall settlement is greater than dry sand. Under the influence of water flow, the surface displacement at the end away from the tunnel face (Y<0m) shows a certain degree of fluctuation. Figure 3(c)-(d) shows the surface uplift when the tunnel moves forward. The amount of surface uplift is small at both ends and large in the middle, and the maximum uplift point is located in the center of the model. Meanwhile, the surface uplift in dry sand is smaller than that in saturated sandy soil.

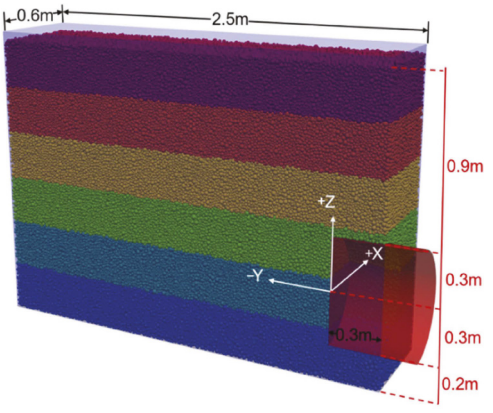

Figure 1. The DEM-CFD model to simulate the progressive failure of tunnel face.

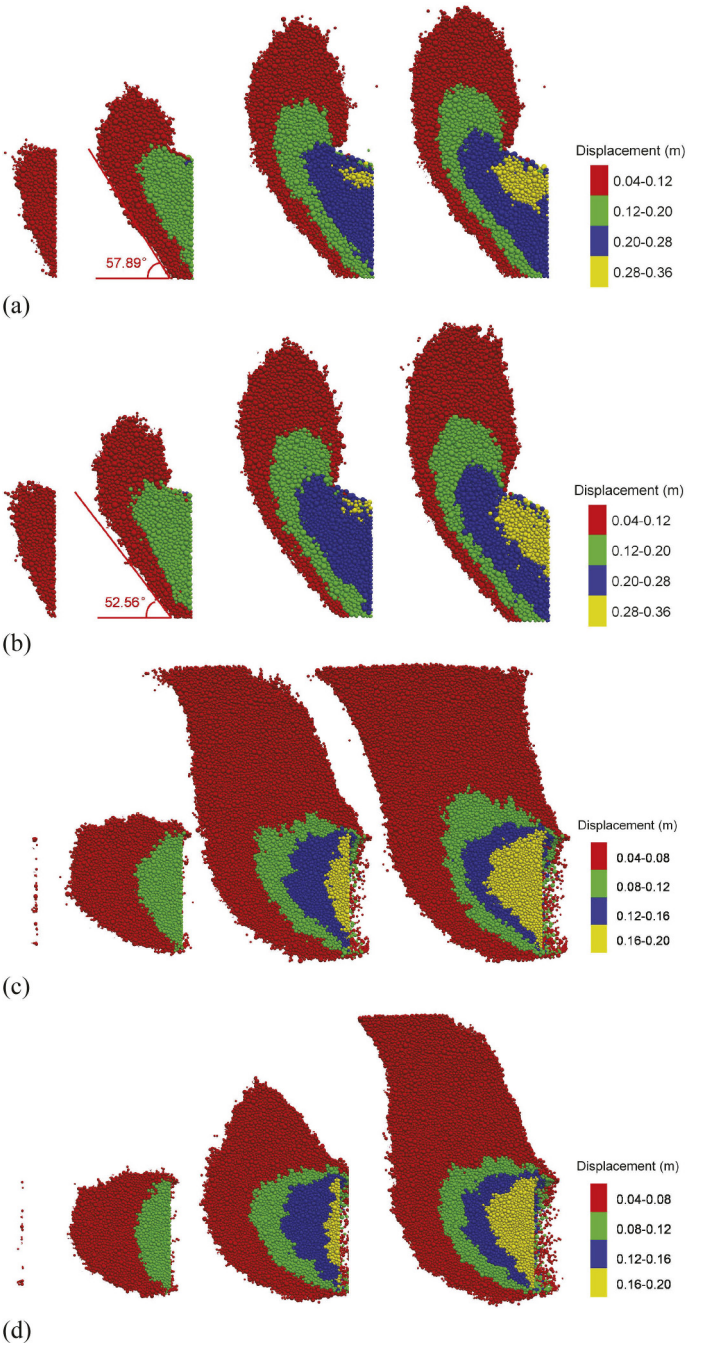

Figure 2. Particle displacement fields from left to right for 40mm, 100mm, 170mm, and 200mm tunnel displacements: (a) Backward displacement in saturated sand (b) Backward displacement in dry sand (c) Forward displacement in saturated sand (d) Forward displacement in dry sand.

3.3 *Supporting force-displacement curve*

The curve of the tunnel face support force versus tunnel displacement is shown in Figure 4, from which it can be seen that under the active damage case, the curve has two stages: the

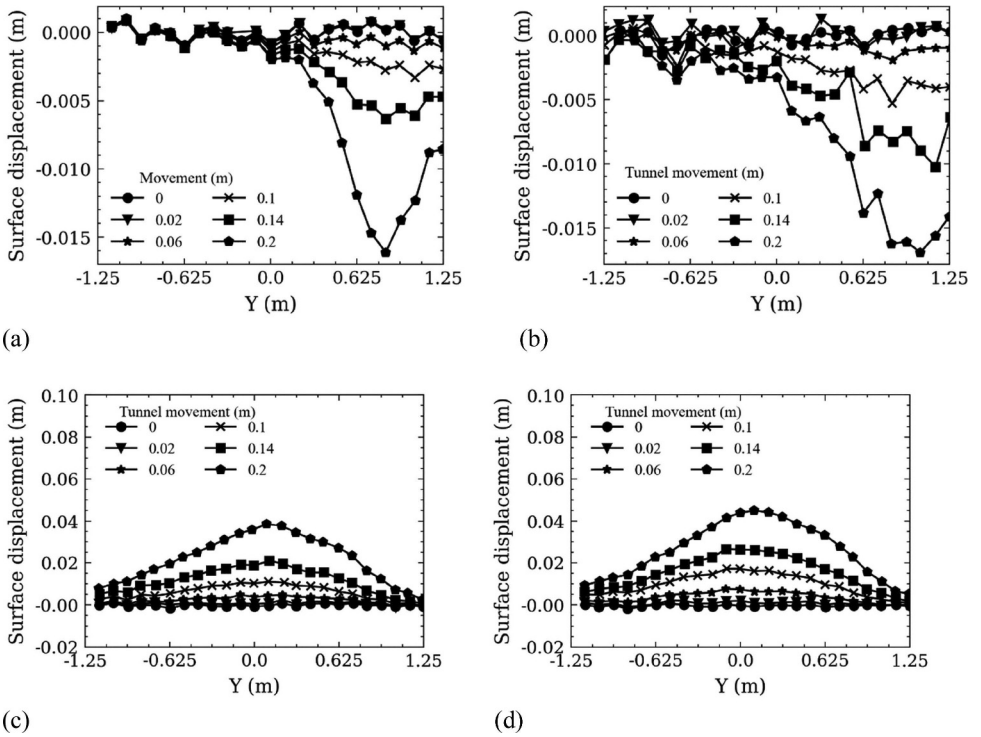

Figure 3. The surface settlement caused by tunnel face: (a) backward movement in dry sand; (b) backward movement in saturated sand; (c) forward movement in dry sand; (d) forward movement in saturated sand.

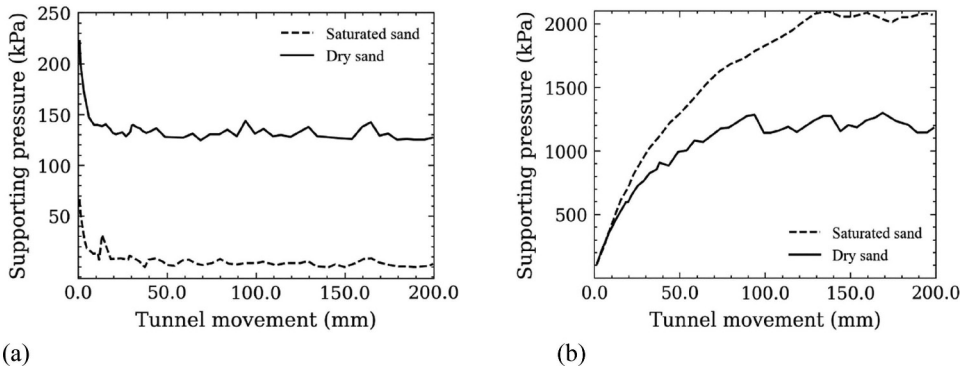

Figure 4. The surface uplift caused by tunnel face: (a) backward movement; (b) forward movement.

support force decreases rapidly with the increase of excavation face displacement in the first stage, and then maintains relative stability in the second stage to reach the ultimate support force. By comparing the two curves corresponding to saturated sand and dry sand, it is found that the ultimate supporting force in saturated sand is significantly higher than that in dry sand. In addition, the support force of dry sand almost decreases to zero, indicating that an arch has formed in the soil. As for the curve of passive damage, the support force is much greater than that for active damage. Unlike the active damage mode, there is no significant steep change in support force but rather a gradual increase to a limiting value as the displacement of the tunnel face increases.

4 CONCLUSION

In this paper, the coupled CFD-DEM method is used to simulate the progressive failure of the tunnel face in saturated sand. Meanwhile, the tunnel face in dry sand is also conducted using DEM as a comparison. Results show that the destabilization angle in saturated sand is slightly larger than that in dry sand for active failure. While in the case of passive damage, the destabilization zone extends to the surface and is significantly larger in saturated sands than in dry sands. In addition, the ultimate support force of the tunnel face for active damage is significantly higher in saturated sand than in dry sand. For passive damage, however, the ultimate support force at the excavation face is higher in dry sand than in saturated sand.

REFERENCES

Kloss, C. *et al*. (2012) 'Models, algorithms and validation for opensource DEM and CFD-DEM', *Progress in Computational Fluid Dynamics*, 12(2–3): 140–152.

Mollon, G., Dias, D. and Soubra, A. (2011) 'Rotational failure mechanisms for the face stability analysis of tunnels driven by a pressurized shield', *International Journal for Numerical and Analytical Methods in Geomechanics*, 35(12): 1363–1388.

Peila, D. (1994) 'A theoretical study of reinforcement influence on the stability of a tunnel face', *Geotechnical & Geological Engineering*, 12(3): 145–168.

Yin, Z. Y., Wang, P. and Zhang, F. (2020) 'Effect of particle shape on the progressive failure of shield tunnel face in granular soils by coupled FDM-DEM method', *Tunnelling and Underground Space Technology*, 100: 103394.